

Motivation

The Southern Ocean is key to global climate because it absorbs large fractions of human-emitted heat and carbon from the atmosphere. The Southern Ocean carbon sink shows significant variability on multiple timescales¹, making it difficult to estimate future trends of CO₂ atmospheric concentration. The rate of carbon uptake depends on the Southern Ocean circulation. Here, to better constrain the timescales of heat and carbon uptake in the Southern Ocean, we study the natural variability generated by eddy-mean flow interactions.

Eddy-mean flow dynamics: theory

The Southern Ocean vigorous eddy field has dynamical similarities with the atmospheric storm track², and its zonal jets are the oceanic analogue of the troposphere's jet stream³. Ambaum and Novak⁴ proposed a two-dimensional dynamical system modelling atmospheric storm track variability. We modify the Ambaum and Novak equations to read:

$$\begin{aligned} X'_0 &= X_1 \\ X'_1 &= -kX_0 - \gamma X_1 + \mathcal{Z}(t) \end{aligned}$$

The original equations have been linearised to a harmonic oscillator of constant k . Additional energy is input by gaussian white noise \mathcal{Z} and removed via linear damping at rate γ . X_0 represents mean flow and X_1 eddy activity. The behaviour of the solution is captured by the phase space and correlation diagrams (fig. 1).

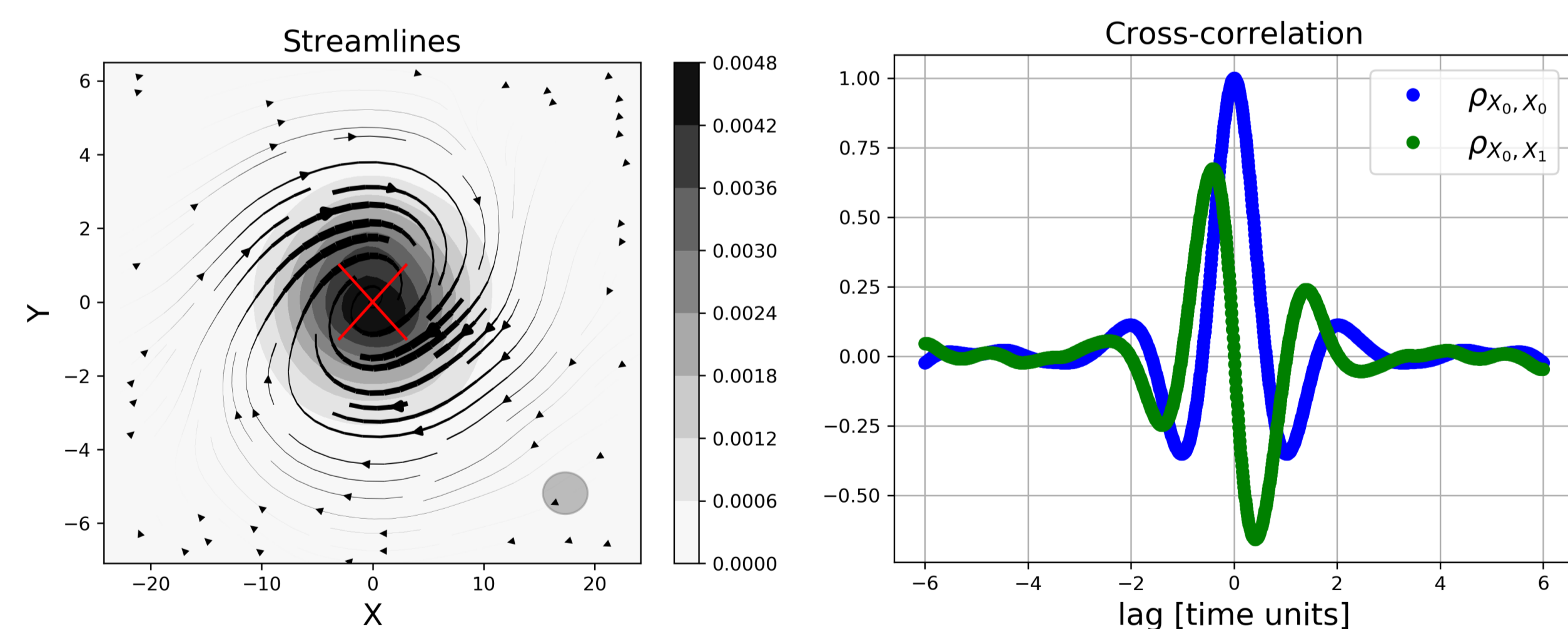


Figure 1: Left: Smoothed phase space diagram; grey shading represents phase space density, black arrows phase space velocity. Right: auto-correlation ρ_{X_0, X_0} (blue) and cross-correlation ρ_{X_0, X_1} (green) functions. Data from a synthetic time-series generated by the modified AN equations

Model

Configuration

- ▶ MITgcm in periodic channel configuration (fig. 2)
- ▶ High horizontal resolution: $\Delta x = 5$ km compared to typical eddy size $L_d \approx 20$ km, with $L_d = NH/f_0$
- ▶ Idealised setup: constant atmospheric forcing, flat bottom topography, no sea-ice, no salinity
- ▶ Reasonable climatology: model configuration gives realistic values for MOC and baroclinic zonal volume transport

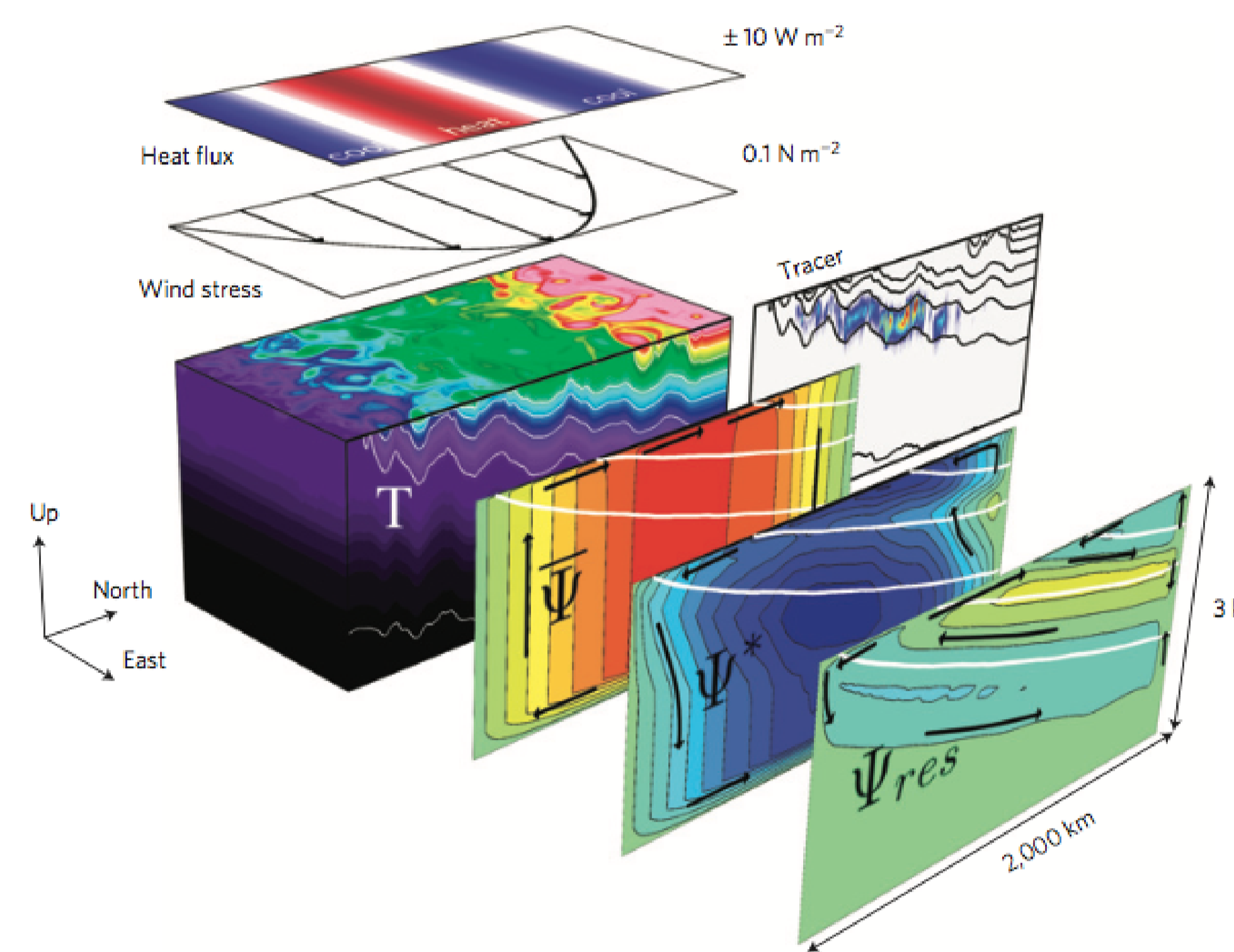


Figure 2: MITgcm in periodic channel configuration⁵ (© Copyright 2011 AMS)

Eddy-mean flow diagnostics

- ▶ Space averages on sub-domain of size comparable with individual jets
- ▶ Mean flow (X_0) described by Eady growth rate, eddy activity (X_1) represented by eddy temperature flux (fig. 3)

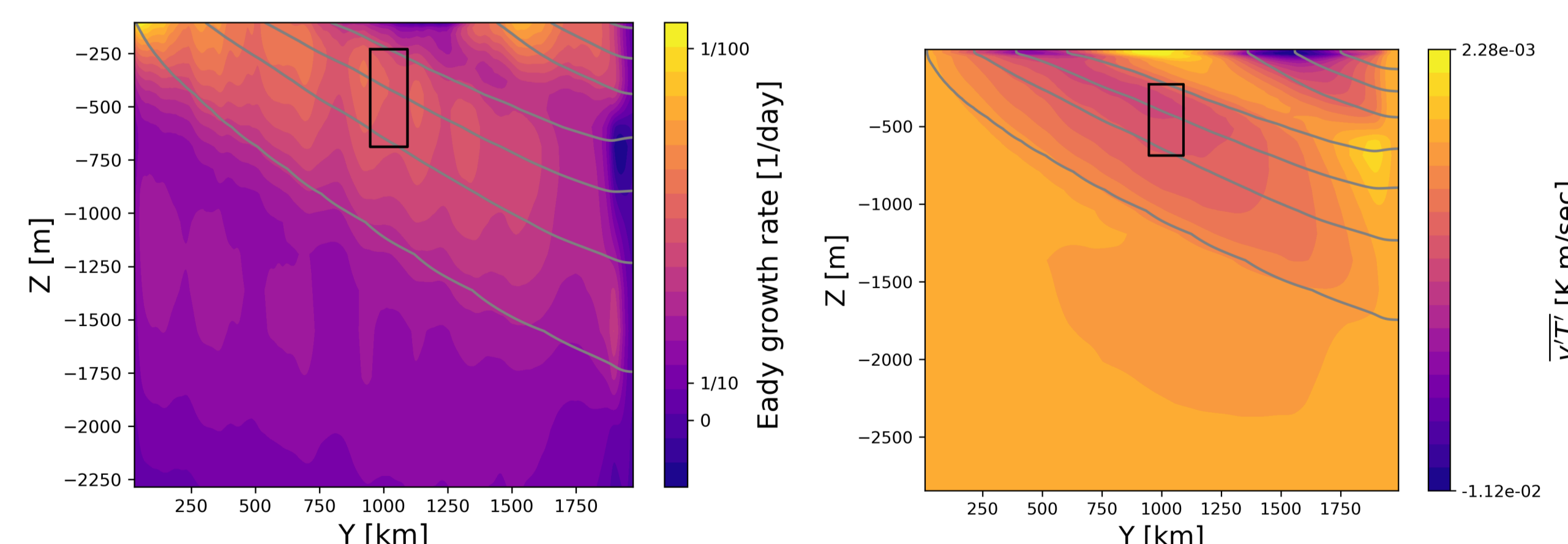


Figure 3: Zonal and time average profiles of Eady growth rate $\sigma = -0.31f\partial_z \bar{u}/N^2$ (left) and eddy temperature flux $\overline{v'T'}$ (right)

Results

- ▶ Modified AN equations capture most features of phase space diagram and correlation plots diagnosed from the MITgcm simulation (fig. 4)

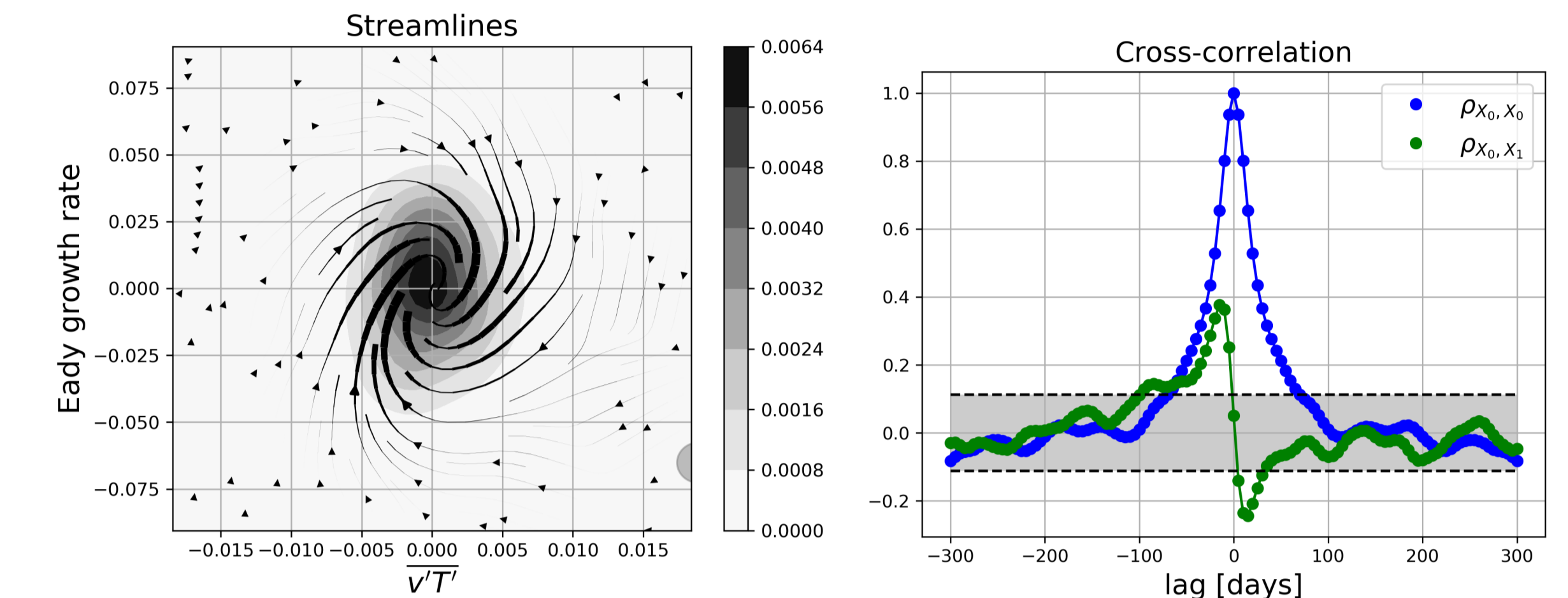


Figure 4: Same as fig. 1, but for MITgcm simulation data. Grey shading in the right plot represents the 95% significance level computed with a correlation t-test

- ▶ Modified AN equations can be discretised to a second order auto-regressive process. Yule-Walker equations use auto-correlation coefficients to estimate physical parameters k and γ :

$$\sqrt{\frac{2\pi}{k}} \approx 77 \text{ day} \quad \gamma \approx 0.8 \text{ day}^{-1}$$

- ▶ Estimated values are broadly consistent with ocean eddy lifecycle and MITgcm linear bottom drag parameter, suggesting that damping time-scale is controlled by interfacial form stress

Conclusions

Summary

- ▶ Mode of eddy-mean flow variability was observed in MITgcm simulation, with no bottom topography and idealised forcing
- ▶ Proposed theoretical model captures most important features of observed fluctuations
- ▶ Future work: test hypothesis on the realistic Southern Ocean State Estimate product⁶

References

- ¹ Gruber, N., et al., Annu. Rev. Mar. Sci. (2019)
- ² Williams, R.G., et al., J. Phys. Oceanogr., 37, 2267-2289 (2012)
- ³ Thompson, A. F., Philos. Trans. R. Soc. A, 366, 4529-4541 (2010)
- ⁴ Ambaum, M. and Novak, L., Q. J. R. Meteorol. Soc., 140, 2680-2684 (2014)
- ⁵ Abernathey, R., et al., J. Phys. Oceanogr., 41, 2261-2278 (2011)
- ⁶ Mazloff, M., et al., J. Phys. Oceanogr., 40, 880-899 (2014)